

Supplementary Material for “Quantum tunneling dynamical behaviour on weakly bond complexes: the case of CO₂-N₂ dimer”

Miguel Lara-Moreno¹, Thierry Stoecklin¹, Philippe Halvick¹, and Majdi Hochlaf²

¹Université de Bordeaux, ISM, CNRS UMR 5255, 33405, Talence, France

²Université Paris-Est, Laboratoire Modélisation et Simulation Multi Echelle, MSME UMR 8208 CNRS, 5 bd Descartes, 77454 Marne-la-Vallée, France

September 3, 2018

1 Theoretical approaches

The 4D-PES model reported by Nasri et al.¹ was incorporated into a 4D variational treatment of the nuclear motions, where the monomers CO₂ and N₂ are considered as rigid rotors. Specifically, the rovibrational energies have been computed using a mixed discrete variable representation-finite basis representation (DVR-FBR) approach. The DVR is based on Sturmian functions to describe the stretching motion along the intermolecular axis, and the FBR is based on coupled angular momentum functions to describe the angular motions (see below).

The variational nature of our method requires an analysis of the convergence in the calculated energies with respect to the size of the basis set. The small rotational constant of the monomers, namely $B_e(\text{CO}_2) = 11698.20 \text{ MHz}^2$ and $B_e(\text{N}_2) = 59905.73 \text{ MHz}^2$,³ the deep potential wells, together with the relatively large reduced mass of the complex make this system extremely memory demanding, i.e. one has to store huge matrices. Although we have employed the truncation-diagonalization approach, one easily reaches the memory limits especially for $J > 0$ where the number of energies to converge rapidly increases. This limitation might affect the final accuracy of the calculated energies. In any case, the final calculations were performed with a rotational basis set conformed by 15 and 8 rotational states of the CO₂ and N₂ respectively. The radial part was described by a 60 points DVR grid in the range 5–20 a_0 . We checked that the absolute value of the variation of the energies was not larger than 0.01 cm^{-1} when any of the parameters of the variational calculation was modified by about 10 %. This allows us to estimate at about $\pm 0.01 \text{ cm}^{-1}$ the error on the calculated energy levels.

The analysis of the rovibrational wavefunctions, symmetry considerations, nuclear spin wavefunctions and spin statistics have been made all over this work leading to numerous results, from the identification of the normal modes to symmetry imposed selection rules and to identification of quantum effects.

2 Bound states calculations

The calculations were performed in the space fixed coordinates $\mathbf{R}(R, \theta, \phi)$, $\hat{\mathbf{r}}_1(\theta_1, \varphi_1)$, $\hat{\mathbf{r}}_2(\theta_2, \varphi_2)$, where \mathbf{R} stand for the intermolecular vector, $\hat{\mathbf{r}}_1$ and $\hat{\mathbf{r}}_2$ are molecular axes vec-

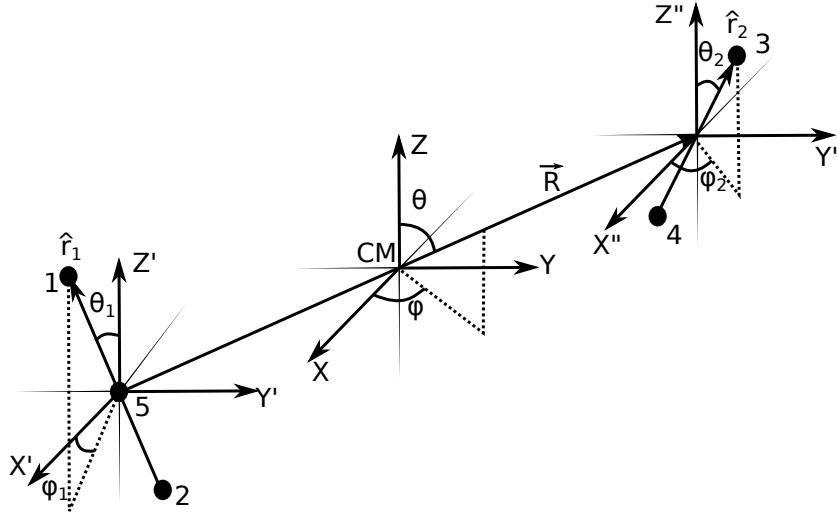


Figure 1: Space fixed coordinates for the $\text{CO}_2\text{-N}_2$ complex. Atoms are labelled as follow, Oxygen: 1-2, Carbon: 5, Nitrogen: 3-4.

tor of CO_2 and N_2 respectively, as shown by Fig. 1. The Hamiltonian of the system in the rigid rotor approximation is

$$\hat{H}(\mathbf{R}, \hat{\mathbf{r}}_1, \hat{\mathbf{r}}_2) = -\frac{\hbar^2}{2\mu} \left[\frac{1}{R} \frac{\partial^2}{\partial R^2} R + \frac{\hat{l}^2}{R^2} \right] + \hat{H}_1(\hat{\mathbf{r}}_1) + \hat{H}_2(\hat{\mathbf{r}}_2) + V(\mathbf{R}, \hat{\mathbf{r}}_1, \hat{\mathbf{r}}_2) \quad (1)$$

where μ is the reduced mass and \hat{H}_i is a linear rigid rotor Hamiltonian whose eigenvalues and eigenfunctions are $\epsilon_{j_i} = B_i j_i(j_i + 1)$ and the spherical harmonics $Y_{j_i m_i}(\hat{\mathbf{r}}_i)$ respectively. B_i are the rotational constants of the linear molecules here set to the experimental values,^{2,3} namely $B_1 = 11698.20$ MHz and $B_2 = 59905.73$ MHz.

The variational Schrödinger equation is then solved using as a basis set the product of a one-dimensional radial functions and angular functions. The most suitable angular functions are the coupled angular momentum functions which take the form

$$|(j_1 j_2) j_{12} l J M\rangle = \sum_{\text{all } m} \langle j_1 m_1 j_2 m_2 | j_{12} m_{12} \rangle \langle j_{12} m_{12} l m_l | J M \rangle \times Y_{j_1 m_1}(\hat{\mathbf{r}}_1) Y_{j_2 m_2}(\hat{\mathbf{r}}_2) Y_{l m_l}(\hat{\mathbf{R}}) \quad (2)$$

These functions are eigenfunctions of the operators J^2 , J_z , j_1^2 , j_2^2 , l^2 , and describe both the global rotation and the internal bending modes of motion of the complex.

A discrete variable representation (DVR) based on the Coulomb Sturmian functions has been employed for describing the stretching motion along the \mathbf{R} vector. These functions are very efficient for reproducing the stretching motion of weakly bonded van der Waals systems as they not only have the proper anharmonic behavior but also provide a sparse DVR grid in the long range. The matrix elements of the kinetics energy operator in this DVR have been recently described in detail.⁴

The $\text{CO}_2\text{-N}_2$ interaction potential¹ is expanded in term of products of spherical harmonics such as

$$V(\mathbf{R}, \hat{\mathbf{r}}_1, \hat{\mathbf{r}}_2) = \sum_{l_1 l_2 l} A_{l_1 l_2 l}(R) \sum_{m_1 m_2 m} \langle l_1 m_1 l_2 m_2 | l m \rangle \times Y_{l_1 m_1}(\hat{\mathbf{r}}_1) Y_{l_2 m_2}(\hat{\mathbf{r}}_2) Y_{l m}^*(\hat{\mathbf{R}}) \quad (3)$$

where the summation is restricted to even values of l_1, l_2, l . This form is less efficient to visualize and compute the angular dependence of the interaction, however it is more convenient for obtaining the mathematical expressions of the matrix elements of the potential in the angular basis set, see Refs. 5,6 for more details. The explicit relation between Eq. 3 and the usual Legendre expansion in body-fixed Jacobi coordinates has been presented by Green.⁶

The final energies are obtained by a sequential diagonalization-truncation procedure.⁷ First, at each point of the radial DVR, the angular part of the Hamiltonian is diagonalized in the angular basis given by Eq. 2, and then truncated by retaining only the eigenfunctions whose eigenvalues are smaller than E_{cut} . Then the product of the radial DVR basis set by the contracted and truncated angular basis set is used to represent and diagonalize the total Hamiltonian given by Eq. 1.

2.1 Symmetry of the CO₂-N₂ vibrational wavefunctions

The symmetry properties of the CO₂-N₂ system are characterized by the G₈ complete nuclear permutation inversion group⁸ which results from the direct product of the permutation group of the indistinguishable oxygen atoms $S_2^{(O)} = \{E, (12)\}$, the permutation group of the indistinguishable N atoms $S_2^{(N)} = \{E, (34)\}$ and the inversion group $\mathcal{E} = \{E, E^*\}$, with the nuclei labeled as defined in Fig. 1. The resulting 8 operations $\{E, (12), (34), (12)(34), E^*, (12)^*, (34)^*, (12)(34)^*\}$ compose the G₈ group. The interaction potential defined by Eq. 3 and the total Hamiltonian defined by Eq. 1 are totally symmetric under all the operations of this group.

Consequently, every rovibrational wavefunction belongs to one of the 8 irreducible representations of the G₈ group. It can be noted that all stretching functions belong to the totally symmetric representation. Therefore, the symmetry of the rovibrational wavefunctions is directly obtained from the irreducible representations to which belong the functions of the rotational basis set. This requires the knowledge of the transformations of the space-fixed coordinates under the G₈ group operations. These transformations are easily derived from Fig. 1 and are given in Table 1.

Table 1: Transformations of the coordinates defined in Fig. 1 and parity of the angular functions defined by Eq. 2 under the operations of the G₈ group

| | θ_1 | φ_1 | θ_2 | φ | θ | φ | R | parity |
|-----------|------------------|-------------------|------------------|-------------------|----------------|-----------------|-----|--------------------|
| E | θ_1 | φ_1 | θ_2 | φ | θ | φ | R | 1 |
| (12) | $\pi - \theta_1$ | $\pi + \varphi_1$ | θ_2 | φ | θ | φ | R | $(-1)^{j_1}$ |
| (34) | θ_1 | φ_1 | $\pi - \theta_2$ | $\pi + \varphi$ | θ | φ | R | $(-1)^{j_2}$ |
| (12)(34) | $\pi - \theta_1$ | $\pi + \varphi_1$ | $\pi - \theta_2$ | $\pi + \varphi$ | θ | φ | R | $(-1)^{j_1+j_2}$ |
| E^* | $\pi - \theta_1$ | $\pi + \varphi_1$ | $\pi - \theta_2$ | $\pi + \varphi$ | $\pi - \theta$ | $\pi + \varphi$ | R | $(-1)^{j_1+j_2+l}$ |
| (12)* | θ_1 | φ_1 | $\pi - \theta_2$ | $\pi + \varphi_2$ | $\pi - \theta$ | $\pi + \varphi$ | R | $(-1)^{j_2+l}$ |
| (34)* | $\pi - \theta_1$ | $\pi + \varphi_1$ | θ_2 | φ_2 | $\pi - \theta$ | $\pi + \varphi$ | R | $(-1)^{j_1+l}$ |
| (12)(34)* | θ_1 | φ_1 | θ_2 | φ_2 | $\pi - \theta$ | $\pi + \varphi$ | R | $(-1)^l$ |

The transformations of the angular basis set, also shown in Table 1, are easily derived by making use of the spherical harmonics properties. The classification of the rovibrational wavefunctions according to the irreducible representations of G₈ are then obtained as a function of the parity of j_1, j_2 , and l as shown in Table 2. These properties can be used to define a symmetry adapted basis set and lead to a considerable reduction of the size of the Hamiltonian matrices to be diagonalized.

Table 2: Classification of the angular basis set functions according to the irreducible representation Γ_i of the G_8 group as a function of the parity, even (e) or odd (o), of j_1 , j_2 , and l .

| j_1 | j_2 | l | Γ_i | j_1 | j_2 | l | Γ_i |
|-------|-------|-----|------------|-------|-------|-----|------------|
| e | e | e | A'_1 | o | e | e | B''_1 |
| e | e | o | A'_2 | o | e | o | B''_2 |
| e | o | e | B'_1 | o | o | e | A''_1 |
| e | o | o | B'_2 | o | o | o | A''_2 |

3 Vibrational normal modes - rigid body model

The rovibrational states of a molecular system can be calculated with the combination of two approximate methods. First, with the harmonic approximation of the PES, reliable for small displacements around the equilibrium geometry, the internal vibrational motions are approximated by the normal modes of motion. Second, if we consider the molecule as a rigid body, the rotational states are easily calculated. The combination of these two approximations has shown to be very useful tool to better understand the results of accurate calculations of fully coupled rovibrational motions.^{9,10} In this approach, the rovibrational wavefunctions of $\text{CO}_2\text{-N}_2$ are defined by a direct product of harmonic oscillator functions and rigid body rotational functions,

$$\Psi_{v_1, v_2, v_3, v_4}^{J_{K_a K_c}} = \prod_i^4 H_{v_i}(\chi_i) \sum_K A_K D_{MK}^J(\alpha, \beta, \gamma) \quad (4)$$

were $J_{K_a K_c}$ are the asymmetric top quantum numbers, v_i the vibrational quantum numbers, H_{v_i} the harmonic oscillator functions, χ_i the normal mode coordinates, and D_{KM}^J the symmetric top functions. The energy level are obtained as

$$E_{v_1, v_2, v_3, v_4}^{J_{K_a K_c}} = hc \sum_i^4 \nu_i \left(v_i + \frac{1}{2} \right) + E_{J_{K_a K_c}}(A, B, C) \quad (5)$$

with ν_i as the normal modes harmonic frequencies given in cm^{-1} , h and c are the Planck and speed of light constants respectively. $E_{J_{K_a K_c}}(A, B, C)$ is the energy of the $J_{K_a K_c}$ level of the asymmetric top as a function of the rotational constants. Analytical expression for $E_{J_{K_a K_c}}(A, B, C)$ can be found elsewhere e.g. Ref. 11.

The use of the latter formula requires the knowledge of the harmonic vibrational frequencies and the rotational constants. Harmonic frequencies are easily calculated within the normal mode analysis which is generally performed with the cartesian coordinates. In the case of the rigid rotor approximation, since some internal coordinates are replaced by constants, the cartesian coordinates cannot be used. Therefore we used the Wilson's FG method¹² which is based on internal coordinates. In the case of a system of two rigid rotors, there is 4 coordinates which are R , θ_1 , θ_2 , $\phi = \varphi_1 - \varphi_2$ as defined in Fig. 1.

The elements of the \mathbf{G} matrix have been determined following the methodology described in Ref. 12. The elements of the force constant matrix \mathbf{F} have been obtained by numerical differentiation. Diagonalization of the matrix \mathbf{FG} matrix lead to the harmonic frequencies and normal modes. Table 3 shows the harmonic normal modes and frequencies obtained for the global (MIN1) and secondary (MIN2) minima of the $\text{CO}_2\text{-N}_2$ complex. The Fig. 2 shows the equilibrium geometry and the inertial axes for these two minima.

On the other hand, the rotational constants can be obtained by the diagonalization of the inertia tensor for each equilibrium geometry. This procedure lead to the following rotational constant, namely $A = 11702.98$ MHz, $B = 2089.74$ MHz, $C = 1773.12$ MHz for the global

Table 3: Harmonic frequencies and normal modes coordinates for the CO₂-N₂ minima.

| Modes | Global | | Secondary | | Orientation | Γ_i |
|-------|------------------|-----------------------------------|------------------|-----------------------------------|--------------|------------|
| | χ_i | $\bar{\nu}_i$ (cm ⁻¹) | χ_i | $\bar{\nu}_i$ (cm ⁻¹) | | |
| v_1 | $\Delta\theta_2$ | 36.9 | $\Delta\theta_1$ | 6.0 | out-of-plane | B_1 |
| v_2 | $\Delta\theta_1$ | 50.7 | $\Delta\theta_2$ | 30.8 | in-plane | B_2 |
| v_3 | ΔR | 58.2 | ΔR | 40.3 | in-plane | A_1 |
| v_4 | $\Delta\theta_2$ | 60.5 | $\Delta\theta_1$ | 10.8 | in-plane | B_2 |

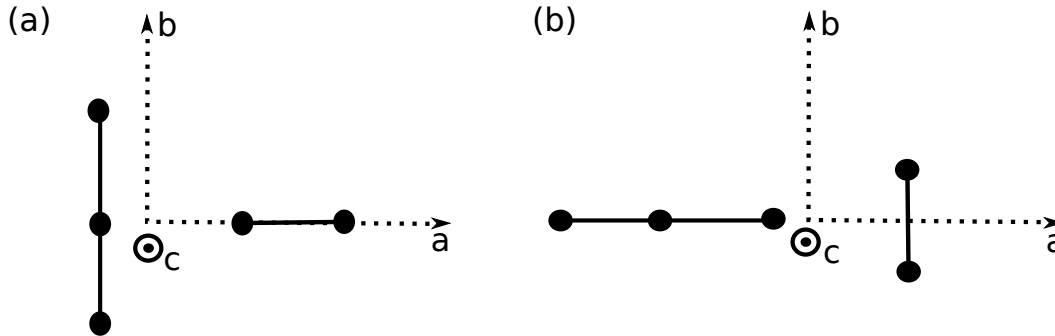


Figure 2: CO₂-N₂ equilibrium geometry for the (a) global (MIN1) and (b) secondary minimum (MIN2). The inertial axes for the complex are labeled so that the moments of inertia follow the order $I_{aa} < I_{bb} < I_{cc}$.

minimum and $A = 60313.50$ MHz, $B = 1826.83$ MHz, $C = 1773.12$ MHz for the secondary minimum.

3.1 Symmetry considerations

The normal coordinates belongs to the representation of the C_{2v} group. It is important to note that the C_{2v} group operations $\{E, C_2(a), \sigma_{ab}, \sigma_{ac}\}$ operates on the vibrational displacements conversely to G_8 operation which permute identical nuclei and has no effect on vibrational displacement. The irreducible representations of C_{2v} to which belong the normal mode coordinates are given in Table 3. The representation to which belongs the total vibrational function is obtained from the direct product of the representations to which belong each of the four normal mode vibrational functions, as shown in Table 4.

Table 4: Classification of the vibrational functions according to the irreducible representation of C_{2v} as a function of the parity, even (e) or odd (o) of the quantum numbers v_1, v_2, v_3, v_4 .

| v_1 | v_2 | v_3 | v_4 | Γ_{vib} | v_1 | v_2 | v_3 | v_4 | Γ_{vib} |
|-------|-------|-------|-------|----------------|-------|-------|-------|-------|----------------|
| e | e | e | e | A_1 | o | e | e | e | B_1 |
| e | e | e | o | B_2 | o | e | e | o | A_2 |
| e | e | o | e | A_1 | o | e | o | e | B_1 |
| e | e | o | o | B_2 | o | e | o | o | A_2 |
| e | o | e | e | B_2 | o | o | e | e | A_2 |
| e | o | e | o | A_1 | o | o | e | o | B_1 |
| e | o | o | e | B_2 | o | o | o | e | A_2 |
| e | o | o | o | A_1 | o | o | o | o | B_1 |

The analysis of the asymmetric top wavefunctions requires the transformation of the Euler angles (α, β, γ) under the element group operations. To determine such transformations we re-

Table 5: Correspondences between the elements of the C_{2v} , D_2 groups and the subgroups of G_8 restricted to the global (MIN1) or the secondary minimum (MIN2). All these groups have the same character table. The representations to which belong the asymmetric top rotational functions are indicated in the last column, depending on the parity of K_a and K_c .

| | (MIN1) | E | (12) | E^* | (12)* | Γ_{rot} |
|--------------|--------|-------|-----------|---------------|---------------|----------------|
| G_8 | (MIN2) | | (34) | | (34)* | |
| C_{2v} | | E | $C_2(a)$ | σ_{ab} | σ_{ac} | $J_{K_a K_c}$ |
| D_2 | | R^0 | R_a^π | R_c^π | R_b^π | |
| | A_1 | 1 | 1 | 1 | 1 | $e e$ |
| Γ_i : | A_2 | 1 | 1 | -1 | -1 | $e o$ |
| | B_1 | 1 | -1 | -1 | 1 | $o o$ |
| | B_2 | 1 | -1 | 1 | -1 | $o e$ |

place each group element of C_{2v} by their equivalent rotation in the D_2 rotation group as shown in Table 5. The symmetry of the rotational wavefunction for a given state $J_{K_a K_c}$ is then determined using the asymmetric top symmetry rules.⁸ The rovibrational wavefunctions are a direct product of the vibrational and rotational functions hence they belong to the representations $\Gamma_{vib} \times \Gamma_{rot}$.

We have now determined to which representations belong the vibrational functions in the limit of small displacements around the equilibrium geometry of the two structures MIN1 and MIN2. Applying the symmetry operation (34) on the structure MIN1, i.e. the permutation of the identical N atoms, we see there is two equivalent structures MIN1. Similarly, with the symmetry operation (12) which permutes identical O atoms, we have also two equivalent structures MIN2. Therefore, the global vibrational wavefunctions are obtained by the combinations of the doubly degenerate local wavefunctions pertaining to the MIN1 or MIN2 structures. The correspondences between the C_{2v} and G_8 irreducible representations are given in the Table 6. These correspondences are determined with the help of the character tables shown in Table 5 and in the appendix.

Table 6: Correspondences between the C_{2v} and G_8 irreducible representations for the two minima.

| C_{2v} | $G_8(\text{MIN1})$ | $G_8(\text{MIN2})$ |
|------------------|----------------------|---------------------|
| $A_1 \oplus A_1$ | $A'_1 \oplus B'_2$ | $A'_1 \oplus B''_2$ |
| $A_2 \oplus A_2$ | $A'_2 \oplus B'_1$ | $A'_2 \oplus B''_1$ |
| $B_1 \oplus B_1$ | $A''_2 \oplus B''_1$ | $A''_2 \oplus B'_1$ |
| $B_2 \oplus B_2$ | $A''_1 \oplus B''_2$ | $A''_1 \oplus B'_2$ |

3.2 Dipole moment operator and selection rules

A given rovibrational transition $i'J' \leftarrow iJ$ will occur with the absorption or emission of a photon only if the matrix elements of the dipole moment operator $\hat{\mu}$ does not vanish. The relative absorption coefficients at a temperature T are proportional to

$$\frac{g_I e^{-E_{i,J}/kT}}{Z(T)} (E_{i',J'} - E_{i,J}) \sum_{M,M',\Omega} |\langle i, J, M | \hat{\mu}_\Omega | i', J', M' \rangle|^2 \quad (6)$$

where $Z(T)$ is the partition function, g_I is the spin-statistical weight and $|i, J, M\rangle$ are the rovibrational bound states functions. Symmetry properties can be used to obtain some useful informations such as the selection rules and the spin-statistical weights.

The dipole moment operator can be expressed in term of the space-fixed coordinates (defined in Fig. 1) by expanding it over the angular functions defined by Eqn. 2,

$$\hat{\mu} = \sum_{\Lambda\Omega\lambda_1\lambda_2\lambda_{12}\lambda_R} C_{\lambda_1\lambda_2\lambda_{12}\lambda_R}^{\Lambda\Omega}(R) |(\lambda_1\lambda_2)\lambda_{12}\lambda_R\Lambda\Omega\rangle, \quad (7)$$

where λ_1 , λ_2 , λ_{12} , λ_R , Λ , Ω are the quantum numbers associated to the operators j_1^2 , j_2^2 , j_{12}^2 , l^2 , J^2 , J_z respectively. Since the dipole moment operator is a first-rank tensor, the later expansion is restrict to $\Lambda = 1$ and $\Omega = 0, \pm 1$. Additional restriction in the expansion coefficients are deduced from the symmetry operations of the G_8 group. First the dipole moment operator must be invariant to any permutation of equivalent nuclei and antisymmetric with respect to inversion. From Table 1 one can easily note that the only non-vanishing term are those with λ_1 and λ_2 even and λ odd. Using the classification given in Table 2 we can conclude that all the components of the dipole moment operator belong to the A'_2 representation. Therefore, the transitions allowed are only those between a pair of rovibrational states for which the product of representations is A'_2 , namely $A'_1 \leftrightarrow A'_2$, $B'_1 \leftrightarrow B'_2$, $A''_1 \leftrightarrow A''_2$, and $B''_1 \leftrightarrow B''_2$. Furthermore, besides the usual $\Delta J = 0, \pm 1$ rule, the following selection rules imposed by symmetry (see Table 2) must also be satisfied : Δj_1 even, Δj_2 even and Δl odd.

3.3 Nuclear spin wavefunction and spin statistics

Although the hyperfine structure is neglected in the present study, the analysis of the nuclear spin states and further the symmetry rules imposed to the rovibrational states via the spin statistics are of great importance since they are closely related to the bands intensity. Let us consider the most abundant isotopes ^{16}O , ^{12}C , ^{14}N whose nuclear spin are $I_{\text{O}} = 0$, $I_{\text{C}} = 0$, $I_{\text{N}} = 1$. Thus CO_2 has only the nuclear spin state $I_{\text{CO}_2} = 0$ while in the case of N_2 three nuclear spin states are possible $I_{\text{N}_2} = 0, 1, 2$. Therefore the spin states of the $\text{CO}_2\text{-N}_2$ complex are $I = 0, 1, 2$. Following the convention used by Frohman et al.,¹³ the species with a nuclear spin $I = 0, 2$ are referred to as *ortho* and those with $I = 1$ as *para*. The quintet ($I = 2$) and the singlet ($I = 0$) spin functions belong to the representation A'_1 of G_8 while the triplet ($I = 1$) spin function belong to B'_1 . According to the Bose-Einstein statistics, the total wavefunction must be symmetric under any permutation of identical nuclei. Therefore the total wavefunction can be only of symmetry A'_1 and A'_2 , as shown by Table A1. Based on the previous statement, the rovibrational states with symmetry A'_1 and A'_2 can be only combined with the A'_1 nuclear spin states (*para*) while those with symmetry B'_1 and B'_2 can be only combined with nuclear spin states B'_2 states (*ortho*). The rovibrational states which belong to the representations A''_1 , A''_2 , B''_1 , and B''_2 are forbidden by the Bose-Einstein statistics. These restrictions are the origin of the statistical weights shown in Table 7, which indicates that the *ortho* intensities are expected to be twice as intense compared with the *para* ones.

Table 7: The statistical weight of the rovibrational states of $\text{CO}_2\text{-N}_2$ in the G_8 group.

| Γ_{rovib} | Stat. weight | Γ_{rovib} | Stat. weight |
|------------------|--------------|------------------|--------------|
| A'_1 | 6 | B'_1 | 3 |
| A''_1 | 0 | B''_1 | 0 |
| A'_2 | 6 | B'_2 | 3 |
| A''_2 | 0 | B''_2 | 0 |

Appendix A The G_8 group

Due to its importance in the present study, we give the character table and the multiplication table of the G_8 group which are not easily found in the literature.

Table A1: Character table of the G_8 group .

| $\Gamma_i :$ | E | $(12)(34)$ | E^* | $(12)(34)^*$ | (12) | (34) | $(12)^*$ | $(34)^*$ |
|--------------|-----|------------|-------|--------------|--------|--------|----------|----------|
| A'_1 | 1 | 1 | 1 | 1 | 1 | 1 | 1 | 1 |
| A''_1 | 1 | 1 | 1 | 1 | -1 | -1 | -1 | -1 |
| A'_2 | 1 | 1 | -1 | -1 | 1 | 1 | -1 | -1 |
| A''_2 | 1 | 1 | -1 | -1 | -1 | -1 | 1 | 1 |
| B'_1 | 1 | -1 | -1 | 1 | 1 | -1 | -1 | 1 |
| B''_1 | 1 | -1 | -1 | 1 | -1 | 1 | 1 | -1 |
| B'_2 | 1 | -1 | 1 | -1 | 1 | -1 | 1 | -1 |
| B''_2 | 1 | -1 | 1 | -1 | -1 | 1 | -1 | 1 |

Table A2: Multiplication table of the G_8 group .

| $\Gamma_i :$ | A'_1 | A'_2 | B'_1 | B'_2 | A''_1 | A''_2 | B''_1 | B''_2 |
|--------------|---------|---------|---------|---------|---------|---------|---------|---------|
| A'_1 | A'_1 | A'_2 | B'_1 | B'_2 | A''_1 | A''_2 | B''_1 | B''_2 |
| A'_2 | A'_2 | A'_1 | B'_2 | B'_1 | A''_2 | A''_1 | B''_2 | B''_1 |
| B'_1 | B'_1 | B'_2 | A'_1 | A'_2 | B''_1 | B''_2 | A''_1 | A''_2 |
| B'_2 | B'_2 | B'_1 | A'_2 | A'_1 | B''_2 | B''_1 | A''_2 | A''_1 |
| A''_1 | A''_1 | A''_2 | B''_1 | B''_2 | A'_1 | A'_2 | B'_1 | B'_2 |
| A''_2 | A''_2 | A''_1 | B''_2 | B''_1 | A'_2 | A'_1 | B'_2 | B'_1 |
| B''_1 | B''_1 | B''_2 | A''_1 | A''_2 | B'_1 | B'_2 | A'_1 | A'_2 |
| B''_2 | B''_2 | B''_1 | A''_2 | A''_1 | B'_2 | B'_1 | A'_2 | A'_1 |

References

- ¹ S. Nasri, Y. Ajili, N.-E. Jaidane, Y. N. Kalugina, P. Halvick, T. Stoecklin, and M. Hochlaf. Potential energy surface of the CO_2N_2 van der Waals complex. *J. Chem. Phys.*, 142(17):174301, 2015.
- ² J. Bendtsen. The rotational and rotation-vibrational raman spectra of $^{14}\text{N}_2$, $^{14}\text{N}^{15}\text{N}$ and $^{15}\text{N}_2$. *J. Raman Spectrosc.*, 2(2):133–145, 1974.
- ³ G. Herzberg. *Molecular spectra and molecular structure. III. Electronic spectra and electronic structure of polyatomic molecules*. Molecular Spectra and Molecular Structure. Van Nostrand, 1966.
- ⁴ M. Lara-Moreno, T. Stoecklin, and P. Halvick. Interaction of rigid $\text{C}_3\text{N}-$ with He: Potential energy surface, bound states, and rotational spectrum. *J. Chem. Phys.*, 146(22):224310, 2017.
- ⁵ H. Klar. Theory of scattering between two rigid rotors. *Z. Phys. A*, 228(1):59–67, 1969.
- ⁶ S. Green. Rotational excitation in $\text{H}_2 - \text{H}_2$ collisions: Closecoupling calculations. *J. Chem. Phys.*, 62(6):2271–2277, 1975.

- ⁷J. C. Light and Z. Bačić. Adiabatic approximation and nonadiabatic corrections in the discrete variable representation: Highly excited vibrational states of triatomic molecules. *J. Chem. Phys.*, 87(7):4008–4019, 1987.
- ⁸P. Bunker. *Molecular Symmetry and Spectroscopy*. Elsevier Science, 2012.
- ⁹J. Tennyson and A. van der Avoird. Quantum dynamics of the van der waals molecule (N₂)₂: An ab initio treatment. *J. Chem. Phys.*, 77(11):5664–5681, 1982.
- ¹⁰H. Chen and J. C. Light. Vibrations of the carbon dioxide dimer. *J. Chem. Phys.*, 112(11):5070–5080, 2000.
- ¹¹R.N. Zare. *Angular momentum: understanding spatial aspects in chemistry and physics*. George Fisher Baker non-resident lectureship in chemistry at Cornell University. Wiley, 1988.
- ¹²E.B. Wilson, J.C. Decius, and P.C. Cross. *Molecular Vibrations: The Theory of Infrared and Raman Vibrational Spectra*. Dover Books on Chemistry. Dover Publications, 2012.
- ¹³D. J. Frohman, E. S. Contreras, R. S. Firestone, S. E. Novick, and W. Klemperer. Microwave spectra, structure, and dynamics of the weakly bound complex, N₂ – CO₂. *J. Chem. Phys.*, 133(24):244303, 2010.